

A Synthetic Approach to Novel Group 13/15 Element Complexes[†]

Eva Leiner and Manfred Scheer*

Institut für Anorganische Chemie der Universität Karlsruhe, D-76128 Karlsruhe, Germany

Received June 17, 2002

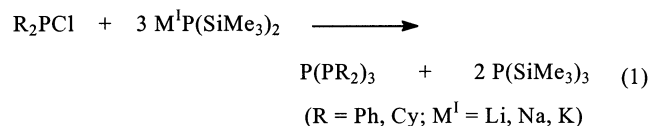
The gallium chloro complex $[\text{GaCl}\{\text{Fe}(\text{CO})_2\text{Cp}\}_2]$ ($\text{Cp} = \eta^5\text{-C}_5\text{H}_5$) was reacted with $\text{KP}(\text{SiMe}_3)_2$ under special conditions to yield the complexes $[\{\text{CpFe}(\text{CO})\}_2\{\mu\text{-(CO)}\}[\mu\text{-Ga}\{\text{CpFe}(\text{CO})_2\}]]$ (**1**) and $[\{\text{CpFe}(\text{CO})_2\}\text{GaP}(\text{SiMe}_3)_4]$ (**2**). Furthermore, $[\{\{\text{CpFe}(\text{CO})_2\}\text{ClGa}(\mu\text{-PPh}_2)_2\text{-FeCpCO}\}]$ (**4**) was obtained by the reaction of $[\text{GaCl}\{\text{Fe}(\text{CO})_2\text{Cp}\}_2]$ with LiPPh_2 . Complexes **1**, **2**, and **4** have been characterized spectroscopically and by X-ray structure analysis. Complex **2** represents an ideal Ga_4P_4 -heterocubane, the first Ga-containing example of this structural type with organometallic substituted group 13 elements. In the solid state compound **4** possesses an almost planar GaPFeP four-membered ring, a novel structural motif in mixed group 13/15 chemistry.

Introduction

The last few decades have witnessed a surge in activity in the area of coordination chemistry of organometallic substituted group 15 elements.¹ One of the challenges in this field is the synthesis of such element ligands² of group 15 elements in combination with main group elements of other groups. While we have already contributed in the synthesis of novel mixed group 15 element ligands³ and also in novel synthetic approaches to mixed group 15/16 element ligands,⁴ the most exciting synthetic challenge is still to stabilize substituent-free oligomers and/or polymers of mixed group 13/15 element ligands in the coordination sphere of transition metals. Previous research of other groups has proven the utility of silyl-phosphines to prepare compounds possessing phosphorus–gallium bonds,^{5,6} like, for example, the synthesis of $[\text{Cl}_2\text{GaP}(\text{SiMe}_3)_2]$ via the reaction of GaCl_3 with $\text{P}(\text{SiMe}_3)_3$. Heterocubane compounds of the general formulas $[\text{RMPr}']_n$ ($\text{R} = \text{organic substituent, M} = \text{Ga, In}$), like, for example, $[\text{iPrGaP}t\text{Bu}]_4$ ⁷ and $[\text{iPrInP}(\text{SiPh}_3)]_4$,⁸ have been prepared recently. Merzweiler et

al. have obtained the In/P heterocubane $[\{\text{CpMo}(\text{CO})_3\}\text{-InP}(\text{SiMe}_3)_4]_9$ via the reaction between $[\text{Cp}(\text{CO})_3\text{MoInCl}_2]$ and $\text{P}(\text{SiMe}_3)_3$. In contrast, Ga compounds of the general type $[(\text{ML}_n)\text{GaPr}']_n$ are not known up to now.

Several synthetic strategies are possible to access the field of naked mixed group 13/15 element ligands.² Among others, one possibility could be to adopt a concept we developed in the past for multiple P–P bond formation reactions.¹⁰ By this method the reaction of $\text{MP}(\text{SiMe}_3)_2$ ($\text{M} = \text{Li, Na, K}$) with diorganochlorophosphines yields *iso*-tetrachlorophosphines of the type $\text{P}(\text{PR}_2)_3$ ($\text{R} = \text{Ph, Cy}$) (eq 1). By using $\text{R}_2\text{P}(\text{S})\text{Cl}$ and $\text{R}_2\text{P}(\text{Cl})\text{ML}_n$ ($\text{ML}_n = \text{M}(\text{CO})_5$; $\text{M} = \text{Cr, W}$), respectively, as the chlorophosphine components, *iso*-tetrachlorophosphines and triphosphines (Scheme 1), respectively, were formed.



Investigations of the reaction pathway showed¹⁰ that the multiple P–P bond formation occurs only if the chlorophosphine component is added dropwise to a solution of alkalimetal-bis(trimethylsilyl)phosphanide cooled to -40°C (Scheme 1). After the first P–P bond formation to give the diphosphine the excess of $\text{M}^1\text{P}(\text{SiMe}_3)_2$ leads to its metalation under formation of a silylated diphosphine and $\text{P}(\text{SiMe}_3)_3$. Subsequent metathesis reaction with the chlorophosphine component and metalation result in triphosphines, which can react further to *iso*-tetrachlorophosphines if the sterics of the chlorophosphine derivative allow. The influence of the alkali metal counterion of $\text{M}^1\text{P}(\text{SiMe}_3)_2$ is decisive only for the completeness of the reaction.

[†] Dedicated to Professor W. Siebert on the occasion of his 65th birthday.

(1) (a) Scheer, M.; Herrmann, E. *Z. Chem.* **1990**, *29*, 41–55. (b) Scherer, O. J. *Angew. Chem.* **1990**, *102*, 1137–1155; *Angew. Chem., Int. Ed. Engl.* **1990**, *29*, 1104–1122. (c) Di Vaira, M.; Stoppioni, P. *Coord. Chem. Rev.* **1992**, *120*, 259–279. (d) Di Vaira, M.; Peruzzini, M.; Stoppioni, P. *Polyhedron* **1987**, *3*, 351–382. (e) Whitmire, K. H. *Adv. Organomet. Chem.* **1998**, *42*, 1–42. (f) Scherer, O. J. *Acc. Chem. Res.* **1999**, *32*, 751–762. (g) Ehse, M.; Romerosa, A.; Peruzzini, M. *Top. Curr. Chem.* **2002**, *220*, 107–140.

(2) Free of any organic substituents or similar fragments such as SiMe_3 , NR_2 , and others.

(3) Umbarkar, S.; Sekar, P.; Scheer, M. *J. Chem. Soc., Dalton Trans.* **2000**, 1135–1137.

(4) Scheer, M.; Umbarkar, S. B.; Chatterjee, S.; Trivedi, R.; Mathur, P. *Angew. Chem.* **2001**, *113*, 399–401; *Angew. Chem., Int. Ed.* **2001**, *40*, 376–378.

(5) Jouet, R. J.; Wells, R. L.; Rheingold, A. L.; Incarvito, C. D. *Organomet. Chem.* **2000**, *601*, 191–198.

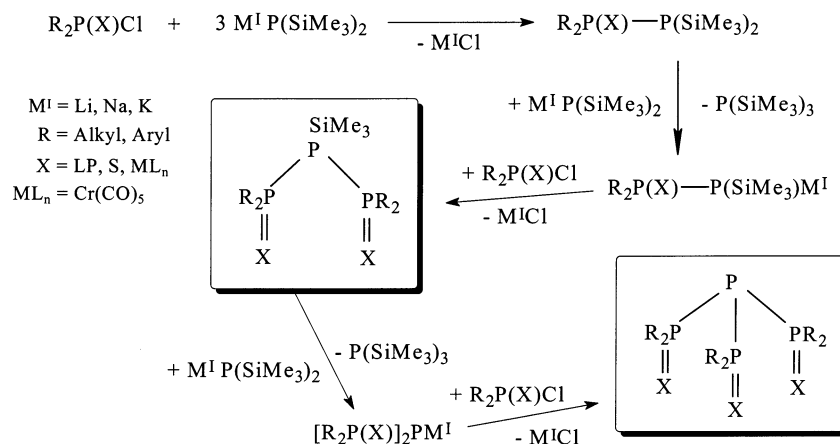
(6) Wiedmann, D.; Hausen, H. D.; Weidlein, J. *Z. Anorg. Allg. Chem.* **1995**, *621*, 1351–1357.

(7) Niediek, K.; Neumüller, B. *Chem. Ber.* **1994**, *127*, 67–71, and compare herein for other heterocubanes of Ga.

(8) Atwood, D. A.; Cowley, A. H.; Jones, R. A.; Mardones, M. A. *J. Organomet. Chem.* **1993**, *449*, C1.

(9) App, U.; Merzweiler, K. *Z. Anorg. Allg. Chem.* **1995**, *621*, 1731–1734.

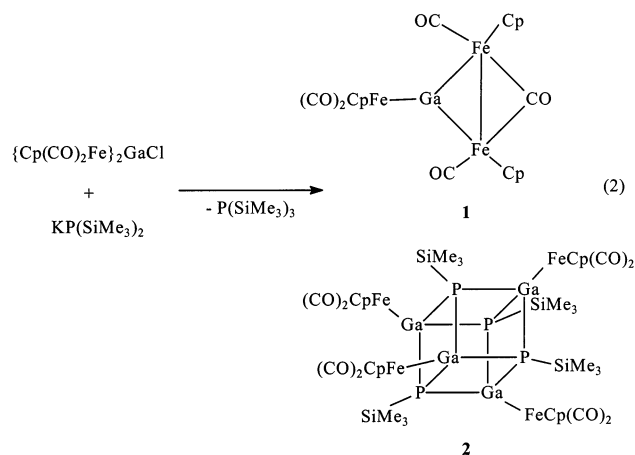
(10) (a) Scheer, M.; Uhlig, F.; Nam, T. T.; Dargatz, M.; Schädler, H.-D.; Herrmann, E. *Z. Anorg. Allg. Chem.* **1990**, *585*, 177–188. (b) Scheer, M.; Gremler, S.; Herrmann, E.; Grünhagen, U.; Dargatz, M.; Kleinpeter, E. *Z. Anorg. Allg. Chem.* **1991**, *600*, 203–210. (c) Scheer, M.; Jones, P. G. *J. Organomet. Chem.* **1992**, *434*, 57–61.

Scheme 1. Reaction Pathway of the Multiple P–P Bond Formation to Form Triphosphines as Well as *iso*-Tetraphosphines


With this synthetic concept in mind compounds of the general type $(ML_n)_2GaCl$ and ML_nGaCl_2 ($ML_n = CpFe(CO)_2$) were reacted with $M^I P(SiMe_3)_2$ ($M^I = Li, K$) under the same special reaction conditions with the aim of preparing organometallic substituted group 13/15 element complexes. The results we are reporting herein.

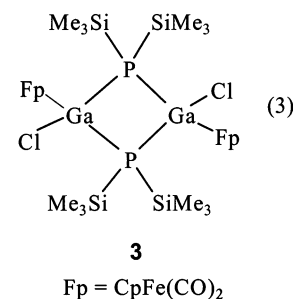
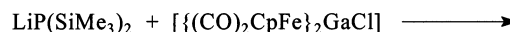
Results and Discussion

Synthesis. Under the above-mentioned reaction conditions $\{Cp(CO)_2Fe\}_2GaCl$ was reacted with $KP(SiMe_3)_2$ at $-40^\circ C$. After the workup, the dinuclear iron complex $[\{CpFe(CO)_2\}_2\{\mu-CO\}[\mu-Ga\{CpFe(CO)_2\}]]$ (**1**) as well as the Ga_4P_4 heterocubane $[\{CpFe(CO)_2\}_4GaP(SiMe_3)_4]$ (**2**) were obtained in almost equal yields (eq 2). Complex **2** represents the first example of a 13/15 heterocubane of gallium where the group 13 element possesses organometallic substituents.

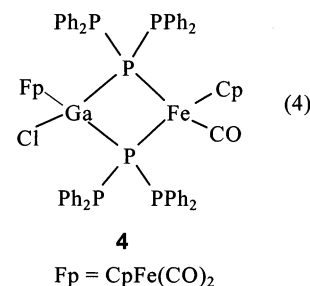
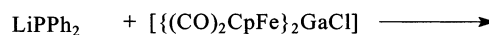


In a similar experiment under the same conditions $\{Cp(CO)_2Fe\}GaCl_2$ was reacted with $KP(SiMe_3)_2$ at $-40^\circ C$. According to the NMR data of the reaction mixture, the same phosphorus-containing compounds were formed as in the reaction with $\{Cp(CO)_2Fe\}_2GaCl$ with more of compound **2**. The $^{31}P\{^1H\}$ NMR spectra of both reaction mixtures reveal signals for $P(SiMe_3)_3$ at -251 ppm, as well as the hydrolysis product $HP(SiMe_3)_2$ at -236.3 ppm, the first one in high quantities. The importance of the chosen reaction conditions (addition of $\{Cp(CO)_2Fe\}_2GaCl$ to a solution of $KP(SiMe_3)_2$ at $-40^\circ C$) is supported by the fact that the reaction of $\{Cp-$

$(CO)_2Fe\}_2GaCl$ with $LiP(SiMe_3)_2$ under inverted conditions (addition of $LiP(SiMe_3)_2$ to a solution of $\{Cp(CO)_2Fe\}_2GaCl$ at $-78^\circ C$)¹¹ leads to the Ga_2P_2 four-membered ring derivative $[\{Cp(CO)_2Fe\}ClGaP(SiMe_3)_2]_2$ (**3**) (eq 3) as the major product without any evidence for the products **1** and **2**. Furthermore, the given chemical shift for **3** at -179.3 ppm could not be detected by $^{31}P\{^1H\}$ NMR at any time for reaction 2.¹¹



Additionally, in a related experiment the reaction of $\{Cp(CO)_2Fe\}_2GaCl$ with $LiPPh_2$ in toluene at low temperatures ($-78^\circ C$) was carried out to give dark orange crystals of $[\{CpFe(CO)_2\}ClGa(\mu-PPh_2)_2FeCpCO]$ (**4**) in 70% yield (eq 4). This result reveals that even while applying the reaction conditions of the multiple P–P bond formation reaction, the use of $LiPPh_2$ leads to $Li-[FeCp(CO)_2]$ elimination reactions without any subsequent metalation reaction.



Spectroscopic Characterization. Complex **1** forms reddish-black, **2** yellow, and **4** orange crystalline products, which are slightly soluble in hexane and readily

soluble in toluene, CH_2Cl_2 , and THF. In their IR spectra CO stretching frequencies are observed typically for terminal CO ligands. For **1** an additional absorption for bridging CO ligands is observed at 1706 cm^{-1} . The CO stretching frequencies of **1** are in a good agreement with those of the *cis*-isomer of $[\text{CpFe}(\text{CO})_2]_2$,¹² where the $\nu(\text{CO})$ of the bridging CO ligand was found at 1777 cm^{-1} . In general, the IR data of **1** and also for *cis*- $[\{\text{CpFe}(\text{CO})_2\}_2(\mu\text{-CO})(\mu\text{-GaCp}^*)]$ ($\nu(\text{CO})_{\text{br}} = 1744\text{ cm}^{-1}$)¹³ indicate a weaker π -acceptor behavior of the RGa moiety in comparison to a CO ligand. Thus, the general feature of Cp^*Ga as a predominant σ -donor in a strongly polarized bond ($\text{Ga}^{\delta+}\text{-M}^{\delta-}$)¹⁴ applies also to the $\text{CpFe}(\text{CO})_2\text{Ga}$ moiety.

Whereas in the EI mass spectra of **1** and **4** the appropriate molecular ion peaks and peaks characterized by the subsequent loss of CO ligands are observed, for **2** the highest mass peak is found to be the molecular ion reduced by one $[\text{CpFe}(\text{CO})_2]$ moiety. The ^1H NMR data of **1** in solution are in accordance with its solid-state structure revealing the η^5 -bonded Cp rings as singlets at 4.34 and 4.29 ppm in the intensity ratio of 2:1. The ^1H NMR data of **2** in solution reveal a singlet at 4.26 ppm for the four η^5 -bound Cp ligands. Additionally a doublet at 0.11 ppm ($^3J_{\text{P,H}} = 4\text{ Hz}$) is observed, revealing the coupling of the SiMe_3 protons with the phosphorus atom. The ^{31}P NMR spectrum of **2** shows a singlet at -53.9 ppm , indicating four equivalent phosphorus atoms of the heterocubane.

The various recorded ^{31}P NMR spectra of the isolated complex **4** in toluene- d_8 right after its resolution and even at low temperatures reveal several peaks and are almost identical with the ^{31}P NMR spectra of the crude reaction mixture. This behavior indicates that in solution fast exchange reactions occur resulting in different homo- and heteronuclear bridged species, and only the low solubility of **4** in contrast to the other species of the solution leads to a reversible crystallization of this product in high yields.

Crystal Structure Analysis. Formally, the structure of **1** can be regarded as a derivative of the dinuclear iron complex $[\text{CpFe}(\text{CO})_2]_2$, where one bridging CO is replaced by a bridging $[\text{CpFe}(\text{CO})\text{Ga}]$ unit (Figure 1). The scrambling process of the ligands in $[\text{CpFe}(\text{CO})_2]_2$ usually favors the *trans*-arrangement of the Cp ligands,¹⁵ whereas the *cis*-complex crystallizes only at low temperatures from its solutions.¹⁶ However, in **1** the assembly of all the ligands, particularly of the $[\text{CpFe}(\text{CO})\text{Ga}]$ moiety, requires a *cis*-arrangement of the Cp ligands at the Fe atoms of the dinuclear $[\text{Cp}_2\text{Fe}_2(\text{CO})_2(\mu\text{-CO})]$ unit, and therefore, the *anti*-arrangement of the Cp ligands seems to be energetically more favorable. We have found the same influence in $[\{\text{CpFe}(\text{CO})_2\}_2(\mu\text{-CO})(\mu\text{-GaCp}^*)]$,¹³ where a Cp^*Ga ligand is bridging the dinuclear Fe complex. The bridging Ga–Fe bond distances in **1** (2.349(2) and 2.370(2) Å) are comparable

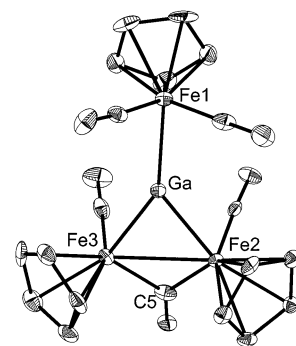


Figure 1. Molecular structure of $[\{\text{CpFe}(\text{CO})_2\}_2\{\mu\text{-CO}\}\mu\text{-Ga}\{\text{CpFe}(\text{CO})_2\}]$ (**1**) in the crystal (showing 30% probability ellipsoids; hydrogen atoms are omitted for clarity). Selected bond lengths (Å) and angles (deg): Ga–Fe(1) 2.332(2), Ga–Fe(2) 2.370(2), Ga–Fe(3) 2.349(2), Fe(2)–Fe(3) 2.655(2), Fe(2)–C(5) 1.903(12), Fe(3)–C(5) 1.933(10), Fe(2)–Ga–Fe(3) 68.49(6), Fe(1)–Ga–Fe(2) 139.50(7), Fe(1)–Ga–Fe(3) 146.91(7), Ga–Fe(2)–Fe(3) 55.37(5), Ga–Fe(3)–Fe(2) 56.14(5), Fe(1)–Fe(3)–Fe(2)–Ga 7.78(0).

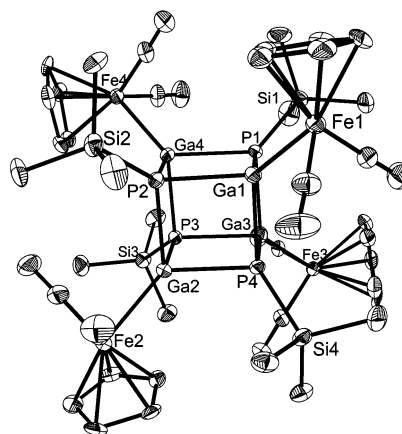


Figure 2. Molecular structure of $[\{\text{CpFe}(\text{CO})_2\}_2\text{GaP}(\text{SiMe}_3)_4]$ (**2**) in the crystal (showing 30% probability ellipsoids; hydrogen atoms are omitted for clarity). Selected bond lengths (Å) and angles (deg): Ga(1)–P(1) 2.438(2), Ga(1)–P(2) 2.418(2), Ga(1)–P(4) 2.428(2), Ga(1)–Fe(1) 2.377(1), P(1)–Si(1) 2.242(3), P(1)–Ga(1)–P(2) 90.35(7), P(1)–Ga(1)–P(4) 90.31(7), P(2)–Ga(1)–P(4) 89.30(7), Ga(1)–P(2)–Ga(4)–P(1) 1.06(1).

with those in the latter complex (2.383(1) and 2.350(1) Å) and therefore close to the lower limit of reported Fe–Ga single bonds (2.29–2.59 Å).¹⁷ However, the exocyclic Ga–Fe1 distance in **1** is shortened (2.332(2) Å). Furthermore, it is remarkable that the exocyclic $\text{CpFe}(\text{CO})_2$ moiety is bent by 12° from the remaining trinuclear Fe₂–Ga unit. The Fe–Fe bond distance (2.655(2) Å) and the Fe1–Ga–Fe2 angle ($68.94(1)^\circ$) of **1** are comparable to those of similar complexes, like, for example, $[\{\text{Fe}(\text{CO})_3\}_2\{\mu\text{-GaSi}(\text{SiMe}_3)_3\}_2(\mu\text{-CO})]$ (2.6804(8) Å)¹⁸ and $[\{\text{CpFe}(\text{CO})_2\}_2(\mu\text{-CO})(\mu\text{-GaMes})]$ (Mes = 2,4,6-trimethylphenyl) (2.6526(6) Å).¹⁷

Complex **2** crystallizes in the acentric orthorhombic space group $P2_12_12_1$, the chirality of which comes from the packing of the molecules in the crystal lattice. The crystal structure analysis of **2** (Figure 2) reveals an almost ideal Ga_4P_4 heterocubane (e.g., the folding angle

(11) Urban App, Ph.D. Thesis, University of Karlsruhe, 1995. The same result was obtained if $\text{KP}(\text{SiMe}_3)_2$ is used at -40°C with the mentioned procedure of addition.

(12) Bullitt, J. G.; Cotton, F. A.; Marks, T. J. *Inorg. Chem.* **1972**, *11*, 671.

(13) Leiner, E.; Scheer, M. *J. Organomet. Chem.* **2002**, *646*, 247.

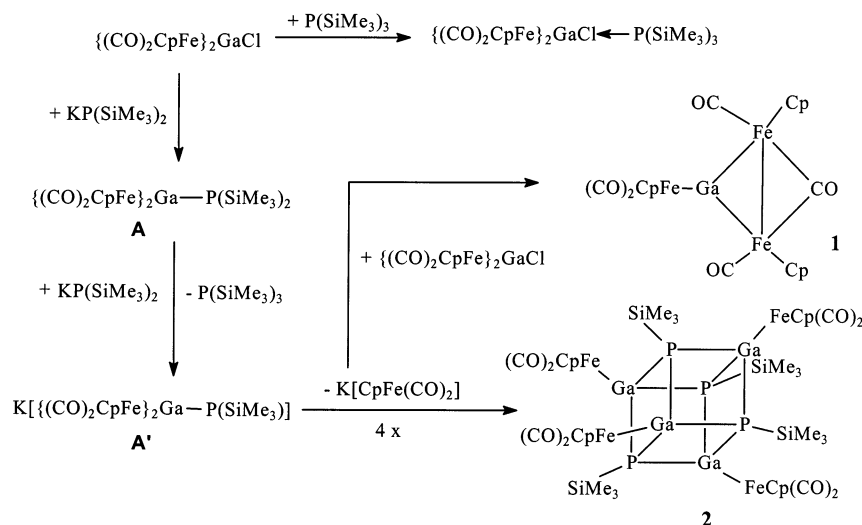
(14) Jutzki, P.; Neumann, B.; Reumann, G.; Stammner, H.-G. *Organometallics* **1998**, *17*, 1305.

(15) Bryan, R. F.; Greene, P. T. *J. Chem. Soc. A* **1970**, 3064–3068.

(16) Bryan, R. F.; Greene, P. T. *J. Chem. Soc. A* **1970**, 3068–3074.

(17) Yamaguchi, T.; Ueno, K.; Ogino, H. *Organometallics* **2001**, *20*, 501–507.

(18) Linti, G.; Koestler, W. *Chem. Eur. J.* **1998**, *4*, 942–949.

Scheme 2. Proposed Reaction Pathway of the Reaction between $\{\text{Cp}(\text{CO})_2\text{Fe}\}_2\text{GaCl}$ and $\text{KP}(\text{SiMe}_3)_2$ 

between the planes P4Ga3P3Ga2 and P1Ga1P2Ga4 is $0.22(5)^\circ$, the average deviation of the atoms of each plane is 0.012 \AA . The average Ga–P bond length in **2** is $2.430(2) \text{ \AA}$ and thus more appropriately compared to the Ga–P distances found in the planar dimers exemplified by $[\text{Cl}_2\text{GaP}(\text{SiMe}_3)_2]_2$ ($2.378(2)$ – $2.380(2) \text{ \AA}$)¹⁹ and $[\text{Me}_2\text{GaP}(\text{SiMe}_3)_2]_2$ (2.448 – 2.451 \AA),²⁰ respectively, or in *cyclo*-trimers such as the planar compound $[\textit{t}\text{Bu}_2\text{GaPH}_2]_3$ (av 2.439 \AA).²¹ In comparison to the organic substituted Ga/P heterocubane $[\textit{t}\text{PrGaP}\textit{t}\text{Bu}]_4$, which reveals slightly shorter Ga–P bond lengths in the range between $2.415(2)$ and $2.425(3) \text{ \AA}$, the regularity of the cubane remains the same. In **2** the average Ga–Fe bond distance of $2.377(1) \text{ \AA}$ is close to the lower limit of the reported Fe–Ga single bonds (2.29 – 2.59 \AA)¹⁷ and is comparable with the exocyclic Fe–Ga distance of **1** ($2.332(2) \text{ \AA}$).

Complex **4** is composed of an almost planar GaPFeP four-membered ring (folding angle between the planes Ga1P2Fe2 and Ga1P1Fe2 is $11.04(6)^\circ$ from planarity), bearing exocyclic Cl, $\text{Cp}(\text{CO})_2\text{Fe}$, SiMe_3 , Cp, and CO ligands (Figure 3). It possesses average Ga–P bond distances of 2.455 \AA , which are similar to those in the four-membered ring compound $[\text{Me}_2\text{GaP}(\text{SiMe}_3)_2]_2$ (2.448 – 2.451 \AA).²⁰ The ring core of **4** is a slightly distorted square with Ga–P–Fe, P–Ga–P, and P–Fe–P bond angles of $97.77(9)^\circ$, $77.84(7)^\circ$, and $86.04(9)^\circ$, respectively. The Fe–Ga bond lengths in **4** are on average $2.260(3) \text{ \AA}$ and therefore shorter than in the strained three-membered ring complex **1** ($2.370(2)$ and $2.349(2) \text{ \AA}$).

Discussion of the Possible Reaction Pathway.

The proposed reaction pathway of the reaction of $[\{\text{Cp}(\text{CO})_2\text{Fe}\}_2\text{GaCl}]$ with $\text{KP}(\text{SiMe}_3)_2$ is shown in Scheme 2 and based on the nature of the isolated products as well as the obtained $^{31}\text{P}\{^1\text{H}\}$ NMR spectroscopic data. In a first step $[\{\text{Cp}(\text{CO})_2\text{Fe}\}_2\text{GaCl}]$ reacts with $\text{KP}(\text{SiMe}_3)_2$ by salt elimination to give product **A** with a Ga–P bond.

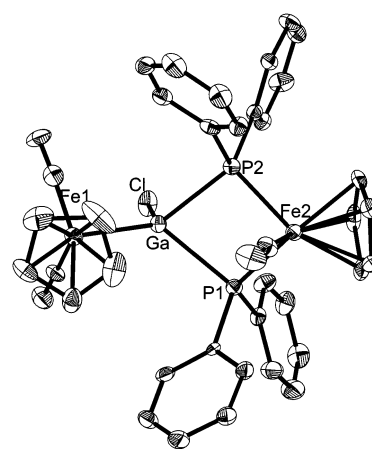


Figure 3. Molecular structure of $[\{\text{CpFe}(\text{CO})_2\}\text{ClGa}(\mu\text{-PPh}_2)_2\text{FeCpCO}]$ (**4**) in the crystal (showing 30% probability ellipsoids; hydrogen atoms are omitted for clarity). Selected bond lengths (\AA) and angles (deg): Ga–P(1) $2.459(3)$, Ga–P(2) $2.450(3)$, Fe(2)–P(1) $2.262(3)$, Fe(2)–P(2) $2.258(3)$, Fe(1)–Ga $2.385(2)$, P(1)–Ga–P(2) $77.84(7)$, P(1)–Fe(2)–P(2) $86.04(9)$, Ga–P(1)–Fe(2) $97.42(8)$, Ga–P(2)–Fe(2) $97.77(9)$, Fe(2)–P(1)–Ga–P(2) $7.10(1)$.

The subsequent nucleophilic attack of the excess $[\text{P}(\text{SiMe}_3)_2]^-$ at a silyl function of the intermediate **A** can be concluded by the high quantities of the NMR-detected $\text{P}(\text{SiMe}_3)_3$. Four equivalents of the thus metallated complex **A'** could react further via $\text{K}[\text{Cp}(\text{CO})_2\text{Fe}]$ elimination to a *cyclo*-dimer and a subsequent tetramer as revealed in the Ga_4P_4 heterocubane $[\{\text{CpFe}(\text{CO})_2\}\text{GaP}(\text{SiMe}_3)]_4$ (**2**). The formation of complex **1** in almost equal isolated yields as **2** indicates the elimination of $\text{K}[\text{Cp}(\text{CO})_2\text{Fe}]$. However, the formation of **1** from the reaction of $\{\text{Cp}(\text{CO})_2\text{Fe}\}_2\text{GaCl}$ with $\text{K}[\text{Cp}(\text{CO})_2\text{Fe}]$ must be more complex, since this reaction leads to the homoleptic complex $[\{\text{Cp}(\text{CO})_2\text{Fe}\}_3\text{Ga}]$, which has been earlier obtained by metathesis reaction starting from GaCl_3 .²² Furthermore, we could state that the reaction of $[\{\text{Cp}(\text{CO})_2\text{Fe}\}_2\text{GaCl}]$ with $\text{P}(\text{SiMe}_3)_3$ leads to the adduct $[\{\text{Cp}(\text{CO})_2\text{Fe}\}_2\text{GaCl}\cdot\{\text{P}(\text{SiMe}_3)_3\}]$ ²³ and some small amounts of **1**, as detected by its crystallographic

(19) Wells, R. L.; Self, M. F.; McPhail, A. T.; Aubuchon, S. R.; Woudenberg, R. C.; Jasinski, J. P. *Organometallics* **1993**, *12*, 2832–2834.

(20) Dillingham, M. D. B.; Burns, J. A.; Byers-Hill, J.; Gripper, K. D.; Pennington, W. T.; Robinson, G. H. *Inorg. Chim. Acta* **1994**, *216*, 267–269.

(21) Cowley, A. H.; Harris, P. R.; Jones, R. A.; Nunn, C. M. *Organometallics* **1991**, *10*, 652–656.

(22) Campbell, R. M.; Clarkson, L. M.; Clegg, W.; Hockless, D. C. R.; Pickett, N. L.; Norman, N. C. *Chem. Ber.* **1992**, *125*, 55–59.

Table 1. Crystallographic Data for Compounds 1, 2, and 4

	1	2 ·2 C ₇ H ₈	4 ·0.5 C ₇ H ₈
formula	C ₂₀ H ₁₅ Fe ₃ GaO ₅	C ₅₄ H ₇₂ Fe ₄ Ga ₄ O ₈ P ₄ Si ₄	C _{40.5} H ₃₄ ClFe ₂ GaO ₃ P ₂
fw	572.59	1587.64	847.49
cryst size, mm	0.15 × 0.05 × 0.02	0.20 × 0.10 × 0.10	0.2 × 0.02 × 0.08
T, K	190(1)	190(1)	193(1)
space group	<i>P</i> 2 ₁ / <i>n</i>	<i>P</i> 2 ₁ 2 ₁ 2 ₁	<i>P</i> 2 ₁ / <i>c</i>
cryst syst	monoclinic	orthorhombic	monoclinic
<i>a</i> , Å	14.699(3)	12.396(3)	10.107(2)
<i>b</i> , Å	10.951(2)	12.396(3)	17.892(4)
<i>c</i> , Å	12.280(3)	44.053(9)	20.907(4)
β, deg	102.45(3)	90.0	99.34(3)
<i>V</i> , Å ³	1930.2(7)	6769(2)	3730.6(13)
<i>Z</i>	4	4	4
<i>d</i> _c , g/cm ³	1.970	1.558	1.509
μ, mm ⁻¹	3.621	2.610	1.679
<i>F</i> (000)	1136	3216	1724
radiation (λ, Å)	0.71073	0.71073	0.71073
diffractometer	STOE IPDS	STOE IPDS	STOE IPDS
2θ range, deg	5.04 ≤ 2θ ≤ 51.86	3.78 ≤ 2θ ≤ 52.08	4.56 ≤ 2θ ≤ 47.98
<i>hkl</i> range	-17 ≤ <i>h</i> ≤ 9, -12 ≤ <i>k</i> ≤ 13, -14 ≤ <i>l</i> ≤ 15	-15 ≤ <i>h</i> ≤ 15, -15 ≤ <i>k</i> ≤ 15, -41 ≤ <i>l</i> ≤ 54	-8 ≤ <i>h</i> ≤ 11, -20 ≤ <i>k</i> ≤ 20, -23 ≤ <i>l</i> ≤ 23
no. of reflns collected	6446	33 348	14 008
ind reflns with <i>I</i> > 2σ(<i>I</i>)	1783 (<i>R</i> _{int} = 0.1050)	11 044 (<i>R</i> _{int} = 0.0506)	2114 (<i>R</i> _{int} = 0.1167)
no. of data/restraints/params	3283/0/262	13060/1/693	6066/0/233
goodness-of-fit on <i>F</i> ²	0.876	1.075	0.723
<i>R</i> ₁ , ^a <i>wR</i> ₂ ^b (<i>I</i> > 2σ(<i>I</i>))	0.0549, 0.1158	0.0568, 0.1362	0.0462, 0.0704
<i>R</i> ₁ , ^a <i>wR</i> ₂ ^b (all data)	0.1132, 0.1330	0.0720, 0.1481	0.1588, 0.0914
largest diff peak, hole, e/Å ³	0.707, -0.820	0.802, -0.726	0.960, -0.410

$$^a R = \sum |F_o| - |F_c| / \sum |F_o|. \quad ^b wR_2 = [\sum w(F_o^2 - F_c^2)^2 / \sum (F_o^2)^2]^{1/2}.$$

unit cell dimensions. The crucial influence of the reaction procedure used for the formation of cubane-like clusters is further supported by the formation of [$\{\text{Cp}(\text{CO})_2\text{Fe}\}\text{ClGaP}(\text{SiMe}_3)_2\}_2$ (**3**), which is obtained by addition of the starting materials in opposite order.

Conclusions

The results have shown that the reaction of $\{\text{Fe}(\text{CO})_2\text{Cp}\}_2\text{GaCl}$ with $\text{KP}(\text{SiMe}_3)_2$ and LiPPh_2 , respectively, leads to the novel group 13/15 element complexes **2** and **4**, both representing novel structural types in element group 13/15 transition metal chemistry, especially for Ga. The present material is not sufficient enough to make conclusions about the efficacy of the applied bond formation concept for group 13/15 chemistry. Nevertheless, it seems to be difficult to replace the last trimethylsilyl substituent at the P atoms via the reaction cascade of reaction 2 since the cubane-like structure found in **2** appears as a kinetically stable geometry in group 13/15 chemistry. In continuation of our efforts in stabilization of naked mixed group 13/15 ligands we will, additionally, increase our efforts in the recent approach in Lewis acid/base-stabilized phosphagallanes and -alanes.²⁴

Experimental Section

General Procedures. All manipulations were performed under an atmosphere of dry Ar using standard Schlenk techniques. All solvents were dried by common methods and freshly distilled prior to use. Gallium trichloride was obtained

(23) $\text{P}(\text{SiMe}_3)_3$ reacts with [$\{\text{Cp}(\text{CO})_2\text{Fe}\}_2\text{GaCl}$] to give a yellow microcrystalline compound showing a chemical shift at -241 ppm in the ³¹P{¹H} NMR spectrum. The crystals were not useful for X-ray structural measurements; however the mass and IR data show the existence of the adduct [$\{\text{Cp}(\text{CO})_2\text{Fe}\}_2\text{GaCl}\{\text{P}(\text{SiMe}_3)_3\}$].

(24) Vogel, U.; Timoshkin, A. Y.; Scheer, M. *Angew. Chem., Int. Ed.* **2001**, *40*, 4409–4412.

commercially and used without further purification. The compounds [$\{\text{CpFe}(\text{CO})_2\}_2\text{GaCl}$],²⁵ $\text{KP}(\text{SiMe}_3)_2$,²⁶ and LiPPh_2 ²⁷ were prepared according to literature methods. NMR spectra were recorded on a Bruker AC 250 (¹H), and the IR spectra were recorded on a Bruker IFS 28. Mass spectroscopy was carried out on a Varian MAT 711 and elemental analysis on a Elementar Vario EL.

Synthesis of [$\{\text{CpFe}(\text{CO})_2\}_2\{\mu\text{-}(\text{CO})\}\{\mu\text{-Ga}\{\text{CpFe}(\text{CO})_2\}\}_2$] (1**) and [$\{\text{CpFe}(\text{CO})_2\}_2\text{GaP}(\text{SiMe}_3)_4$] (**2**).** [$\{\text{CpFe}(\text{CO})_2\}_2\text{GaCl}$] (0.235 g, 0.5 mmol) was added to a slurry of $\text{K}(\text{PSiMe}_3)_2$ (0.110 g, 0.5 mmol) in toluene (10 mL) at -40 °C. The reaction mixture was allowed to warm and stirred for 2 h further at room temperature. After filtering, the resulting red-brown solution was reduced to 2 mL and stored at -30 °C. After a few days small reddish-black crystals of [$\{\text{CpFe}(\text{CO})_2\}_2\{\mu\text{-}(\text{CO})\}\{\mu\text{-Ga}(\text{CpFe}(\text{CO})_2)_2\}$] (**1**) (yield 0.115 g, 40% with respect to gallium) and big yellow crystals of [$\{\text{CpFe}(\text{CO})_2\}_2\text{GaP}(\text{SiMe}_3)_4$] (**2**) (yield 0.210 g, 30% with respect to gallium) are formed, which were filtered and dried under vacuum. The products can be separated by selection of the crystals under a microscope in a glovebox. Data for **1**: Anal. Calcd for C₂₀H₁₅Fe₃GaO₅: C, 41.95; H, 2.64. Found: C, 41.63; H, 2.26. ¹H NMR (C₆D₆, 301 K): δ 4.34 (s, 10 H, Cp, [$\text{CpFe}(\text{CO})_2$]), 4.29 (s, 5 H, Cp, [$\text{CpFe}(\text{CO})_2$]). IR (cm⁻¹, KBr): 1985(s), 1938(s), 1900(s,-br), 1866(m), 1706(m). MS (EI, 70 eV): *m/z* (%) 572 (31) [M^+], 544 (35) [$\text{M}^+ - \text{CO}$], 516 (17) [$\text{M}^+ - 3(\text{CO})$], 460 (52) [$\text{M}^+ - 4(\text{CO})$], 432 (87) [$\text{M}^+ - 5(\text{CO})$], 186 (100) [$\text{M}^+ - 5(\text{CO}) - \text{Fe} - \text{Ga} - \text{Cp}$], 177 (5) [$\{\text{CpFe}(\text{CO})_2\}^+$], 69 (69) [Ga^+]. Data for **2**: ¹H NMR (C₆D₆, 301 K): δ 4.26 (s, 20 H, Cp), δ 0.11 (d, 36 H, SiMe₃, ³*J*_{P-H} = 4 Hz). ³¹P NMR (C₆D₆, 301 K): δ -53.95. IR (cm⁻¹, KBr): 1971(s), 1929(s,br). MS (EI, 70 eV): *m/z* (%) 1227 (1) [$\text{M}^+ - \{\text{CpFe}(\text{CO})_2\}$], 306 (1) [$\{\text{CpFe}(\text{CO})_2\}\text{GaP}(\text{SiMe}_3)_4^+$].

Synthesis of [$\{\text{CpFe}(\text{CO})_2\}_2\text{ClGa}(\mu\text{-PPh}_2)_2\text{FeCpCO}$] (4**).** [$\{\text{CpFe}(\text{CO})_2\}_2\text{GaCl}$] (0.235 g, 0.5 mmol) was added to a slurry of LiPPh_2 (dioxane) (0.140 g, 0.5 mmol) in toluene (30

(25) Borovik, A. S.; Bott, S. G.; Barron, A. R. *Organometallics* **1999**, *18*, 2668–2676.

(26) Uhlig, F.; Hummeltenberg, R. *J. Organomet. Chem.* **1993**, *452*, C9–C10.

(27) Klein, H. F.; Gass, M.; Zucha, U.; Eisenmann, B. *Z. Naturforsch. B* **1988**, *43*, 927–932.

mL) at $-78\text{ }^{\circ}\text{C}$. The resulting red-brown reaction mixture was allowed to warm and stirred for 2 h further at room temperature. After filtering, the solution was reduced to 2 mL and stored at $-30\text{ }^{\circ}\text{C}$. After a few days orange crystals of **4** could be isolated (yield 0.297 g, 70% with respect to gallium). Data for **4**: Anal. Calcd for $\text{C}_{20}\text{H}_{15}\text{Fe}_3\text{GaO}_5$: C, 55.45; H, 3.77. Found: C, 55.03; H, 3.34. IR (cm^{-1} , KBr): 1978(s,br), 1938(s), 1919(s). MS (EI, 70 eV): m/z (%) 800 (7) $[\text{M}^+]$, 772 (2) $[\text{M}^+ - \text{CO}]$, 625 (65) $[\text{M}^+ - \text{Fe} - 2(\text{CO}) - \text{Cp}]$, 491 (69) $[\text{CpFe}\{\text{P}(\text{Ph})_2\}_2]^+$, 306 (100) $[\text{CpFe}\{\text{P}(\text{Ph})_2\}]^+$, 268 (3) $[(\text{CO})\text{Fe}\{\text{P}(\text{Ph})_2\}]^+$, 239 (27) $[\text{Fe}\{\text{P}(\text{Ph})_2\}]^+$, 185 (17) $[\text{P}(\text{Ph})_2]^+$, 108 (14) $[\text{PPh}]^+$, 69 (22) $[\text{Ga}]^+$. ^{31}P NMR (C_7D_8 , 301 K): δ 30.8, 34.6 (ratio 2:1) (cf. discussion above).

Crystal Structure Analysis. Crystal structure analyses were performed on a STOE IPDS diffractometer using Mo $K\alpha$ ($\lambda = 0.71069\text{ \AA}$) radiation. Machine parameters, crystal data, and data collection parameters are summarized in Table 1. The structures were solved by direct methods using SHELXS-97^{28a} and refined using the method of least-squares refinement on F^2 in SHELXL-97.^{28b} All non-hydrogen atoms were refined

(28) (a) Sheldrick, G. M. *SHELXS-97*; University of Göttingen, 1998.
(b) Sheldrick, G. M. *SHELXL-97*; University of Göttingen, 1997.

anisotropically. Hydrogen atoms were fixed in calculated positions and were refined isotropically. For **2** the distance between the atoms C(47) and C(41) of one of the toluene molecules in the crystal lattice must be fitted together by a DFIX command. Complex **2** crystallizes in the acentric space group $P2_12_12_1$ as an enantiomeric pure compound [flack parameter = $-0.007(15)$]. For **4** the toluene molecule was found to be disordered, and these C atoms were solely refined isotropically.

Acknowledgment. The authors thank the Deutsche Forschungsgemeinschaft and the Fonds der Chemischen Industrie for comprehensive financial support. E.L. is grateful for a Ph.D. fellowship of the Fonds der Chemischen Industrie.

Supporting Information Available: Complete tables of crystal data, atomic coordinates, H atom parameters, bond distances, and anisotropic displacement parameters and fully labeled figures for **1**, **2**, and **4**. This material is available free of charge via the Internet at <http://pubs.acs.org>.

OM020473+